Open access • Journal Article • DOI:10.1179/026708301101510348

# Design of novel high strength bainitic steels: Part 1 — Source link

Francisca García Caballero, H. K. D. H. Bhadeshia, K. J. A. Mawella, D. G. Jones ...+1 more authors

**Institutions:** University of Cambridge

**Published on:** 01 May 2001 - Materials Science and Technology (Taylor & Francis)

**Topics:** Austenite, Hardenability, Continuous cooling transformation and Toughness

# Design of novel high-strength bainitic steels. Part I

F. G. Caballero, H. K. D. H. Bhadeshia, K. J. A. Mawella, D. G. Jones and P. Brown

Dr F. G. Caballero and Professor H. K. D. H. Bhadeshia are in the Department of Materials Science and Metallurgy, University of Cambridge, Pembroke Street, Cambridge CB2 3QZ, UK. Dr K. J. A. Mawella, D. G. Jones and Dr P. Brown are in the Structural Materials Centre, Defence Evaluation Research Agency, R1079, Bldg A7, Farnborough GU14 0LX, UK

Mixed microstructures consisting of fine plates of upper bainitic ferrite separated by thin films of stable retained austenite have seen many applications in recent years. There may also be some martensite present although carbides are avoided by the judicious use of silicon as an alloying element. The essential principles governing the optimisation of such microstructures are well established, particularly that large regions of unstable high-carbon retained austenite must be avoided. With careful design, impressive combinations of strength and toughness have been reported for high-silicon bainitic steels. The aim of the present work was to see how far these concepts can be extended to achieve the highest ever combination of strength and toughness in bulk-samples subjected to continuous cooling transformation, consistent with certain hardenability and processing requirements. Thus, Part I of this study deals with the design, using phase transformation theory, of a series of bainitic alloys, given a set of industrial constraints.

# 1 Introduction

High-strength bainitic steels have not in practice been as successful as quenched and tempered martensitic steels, because the coarse cementite particles in bainite are detrimental to toughness. However, the precipitation of cementite during bainitic transformation can be suppressed by alloying the steel with about 1.5 wt-% of silicon, which has very low solubility in cementite and greatly retards its growth from austenite.[1-12] The carbon that is rejected from the bainitic ferrite enriches the residual austenite, thereby stabilising it down to ambient temperature. The resulting microstructure consists of fine plates of bainitic ferrite separated by carbon-enriched regions of austenite.

This mixed microstructure is in principle an ideal combination from many points of view. In particular, the steel has a high resistance to cleavage fracture and void formation due to the absence of fine carbides. There is then a possibility of improving simultaneously the strength and toughness because of the ultrafine grain size of the bainitic ferrite plates, and of further enhancing the toughness by a transformation-induced plasticity effect.

In spite of all these potential advantages, the bainitic ferrite-austenite microstructure has on many occasions failed to live up to its promise, primarily because of the instability of relatively large or blocky regions of austenite which become trapped between sheaves of bainite.[8,13] The blocks of austenite tend to transform to high carbon, untempered martensite under the influence of small stresses and consequently have an embrittling effect. On the contrary, the films of austenite that are trapped between the platelets of ferrite in a sheaf are much more stable, partly

because of their higher carbon concentration, but also because of the constraint to transformation from the surrounding plates of ferrite.

Therefore, every effort has to be made to reduce the fraction of blocky austenite present in the microstructure and increase its stability to martensitic transformation. The aim of alloy design should then be to increase the maximum permitted degree of transformation to bainitic ferrite. There may be other constraints, for example, the need to ensure that the hardenability of the steel is sufficient for industrial production.

There are applications in the defence industries where secondary hardened martensitic steels are used in the manufacture of large components shaped by forging. The minimum strength and toughness required are 1100 MPa and 125 MPa$\sqrt{m}$. This has never been achieved with the mixed microstructures of bainite and austenite. The aim of the present work was to see how far the concepts of bainite transformation theory can be exploited to achieve the highest ever combination of strength and toughness in bulk samples subjected to continuous cooling transformation, consistent with certain hardenability and processing requirements. Part I of this study deals with the design, using phase transformation theory, of a series of bainitic alloys, given a set of industrial constraints. Part II is concerned with experimental verification of the design process.

## 2 Modelling of microstructure and properties

### 2.1 IMPROVEMENT OF TOUGHNESS, THE $T_o'$ CURVE

The bainite transformation progresses by the diffusionless growth of tiny platelets known as "sub-units". The excess carbon in these platelets partitions into the residual austenite soon after the growth event. Diffusionless growth of this kind can only occur if the carbon concentration of the residual austenite is below that given by the $T_o'$ curve. The $T_o$ curve is the locus of all points, on a temperature versus carbon concentration plot, where austenite and ferrite of the same chemical composition have the same free energy. The $T_o'$ curve is defined similarly but taking into account the stored energy of the ferrite due to the displacive mechanism of transformation. It follows that the maximum amount of bainite that can be obtained at any temperature is limited by the fact that the carbon content of the residual austenite must not exceed the $T_o'$ curve on the phase diagram.[14-17]

The $T_o'$ concept can be used to optimise the mechanical properties by minimising blocky, unstable austenite.[8,9] An increase in the amount of bainitic ferrite in the microstructure is needed in order to consume the blocks of austenite.

The variation of the carbon content of austenite, $x_\gamma$ as a function of the average carbon content of the alloy, $\bar{x}$, and the volume fraction of bainitic ferrite $V_b$ is given by,[7]

$$x_\gamma = \bar{x} + V_b \frac{(\bar{x} - s)}{(1 - V_b)} \quad (1)$$

where $s$ is the amount of carbon trapped in the bainitic ferrite, either in solid solution ($s$ = 0.03 wt-%), or in the form of carbides ($s$ = 0.27 wt-%).

Previous work[7,14] suggested two main methods of increasing the maximum permitted degree of transformation to bainitic ferrite:

– by reducing the overall carbon content $\bar{x}$ of the alloy concerned, so that the critical concentration in the austenite at which displacive transformation becomes impossible is reached at a later stage (and hence a higher $V_b$) in the transformation (equation (1)). Of course, this is only useful if the reduction of the overall carbon content of the alloy does not at the same time lead to a decrease in the strength of the microstructure.
– by modifying the substitutional alloying elements such that the $T_o'$ curve is shifted to higher austenite carbon concentrations.[7,8,14]

## 2.2 TIME-TEMPERATURE TRANSFORMATION (TTT) DIAGRAMS

Apart from controlling the $T_o'$ curve, substitutional solutes also affect hardenability which is an important design parameter since industrial manufacturing generally involves continuous cooling transformation. For this purpose, we use a thermodynamic method[18] developed to allow the estimation of isothermal transformation diagrams, from a knowledge of the chemical composition of the steel concerned.

The TTT diagram is treated as being composed of two overlapping 'C' curves, one representing the diffusional ferrite and pearlite transformations, and the other representing the displacive Widmanstätten ferrite and bainite reactions. It is possible to predict relative shifts in these component curves, as a function of alloying element content, thus making the technique potentially useful in the theoretical steel design.

## 2.3 DEFORMATION MODEL FOR THREE-PHASE ALLOYS

As a further step, a model for calculating the strength of the mixed microstructure has been developed as an aid in the design process.

In a multiphase alloy, each phase contributes to the overall properties of the aggregate. If the contributions from each phase are independent, then the properties of the multiphase alloy will be a weighted average of the properties of the individual phase. However, the properties of the aggregate may be influenced by interactions amongst the phases. Two simple models, equal strain and equal stress, have often been employed to estimate the flow curve of a two-phase alloy from those of the constituent phases.[19] Sometimes composites of the above two models have also been considered.[20,21] However, these models are not based on a detailed consideration of solid mechanics.

In this work, we have attempted to calculate the stress / strain curve of a microstructure consisting of bainitic ferrite separated by carbon-enriched regions of austenite and some martensite. This three-phase microstructure has, for the purposes of calculations, been treated as a mixture of two phases, a hard phase consisting of bainite and martensite, and a soft phase, which is austenite.

One model successfully used to obtain the deformation parameters of two-phase alloys is that of Tomota et al. where the internal stresses produced by the inhomogeneous distribution of plastic strain are taken into account.[22] Furthermore, the stress and strain distributions in the component phases can be followed at every stage of the deformation process. It is assumed that the true stress ($\sigma$) / true strain ($\varepsilon$) behaviour of the mixed microstructure and of the component phases can be represented by a power law of the form

$$\sigma = K\varepsilon^{n} \qquad (2)$$

where $K$ is the strength coefficient and $n$ is the strain hardening coefficient.

The applied stress before the onset of plastic deformation in the hard phase is given as

$$\sigma_m = \sigma_s\left(\frac{\varepsilon_m}{1-f}\right) + \frac{f}{1-f}A\varepsilon_m \tag{3}$$

with

$$\varepsilon_m = (1-f)\varepsilon_s \qquad \text{and} \qquad A = \frac{E(7-5\nu)}{10\left(1-\nu^2\right)} \tag{4}$$

where $\sigma_m$ and $\varepsilon_m$ are the true stress and true plastic strain, respectively in the material as a whole, $f$ is the volume fraction of the harder phase (bainite + martensite), $\sigma_s$ is the true flow stress of the soft phase, $E$ is Young's modulus, taken to be 210 GPa and $\nu$ is Poisson's ratio, taken to be 0.33.

The onset of plastic flow in the harder phase is represented by the following set of simultaneous equations

$$\sigma_m^c = \sigma_s\left(\frac{\varepsilon_m^c}{1-f}\right) + \frac{f}{1-f}A\varepsilon_m^c \tag{5}$$

$$\sigma_m^c = \sigma_{ho} - A\varepsilon_m^c \tag{6}$$

where $\sigma_m^c$ and $\varepsilon_m^c$ are the critical true stress and plastic strain, respectively to start yielding in the harder phase, and $\sigma_{ho}$ is the true yield stress for the harder phase.

Further deformation is calculated for small strain increments from the following simultaneous equations

$$\sigma_s\left(\frac{\varepsilon_m^c}{1-f}+\delta\varepsilon_s\right)=\sigma_m-fA\left[\frac{\varepsilon_m^c}{1-f}+\delta\varepsilon_s-\delta\varepsilon_h\right] \tag{7}$$

$$\sigma_h(\delta\varepsilon_h)=\sigma_m+(1-f)A\left[\frac{\varepsilon_m^c}{1-f}+\delta\varepsilon_s-\delta\varepsilon_h\right] \tag{8}$$

where $\sigma_h$ is the true flow stress of hard phase, and $\delta\varepsilon_s$ and $\delta\varepsilon_h$ are strain increments in soft and hard phases, respectively.

Thus the complete stress / strain curve for the mixed microstructure can be computed. However, this mathematical procedure can only be applied if the true stress / true strain relations (equation (2)) of the component phases are known.

Young and Bhadeshia calculated the strength of a mixed microstructure of bainite and martensite, including constraint effects and changes in martensite composition (and hence strength) as bainite forms.[23] According to them the strength of martensite and bainite as individual phases can be factorised into a number of intrinsic components

$$\sigma=\sigma_{Fe}+\sum\sigma_{ss,i}+\sigma_C+K_L\left(\bar{L}_3\right)^{-1}+K_D\rho_D^{1/2} \tag{9}$$

where $K_L$ and $K_D$ are constants, $\sigma_{Fe}$ is the strength of pure annealed iron, $\sigma_{ss,i}$ is the solid solution strengthening due to substitutional solute $i$, $\sigma_C$ is the solid solution strengthening due to carbon, $\bar{L}_3$ is a measure of the ferrite plate size, and $\rho_D$ is the dislocation density.

In addition, the strength of constrained bainite may be represented by the equation

$$\sigma_B \approx \sigma'_B\left[0.65\,exp\left(-3.3V_B\right)+0.988\right] \leq \sigma_M \tag{10}$$

where $\sigma_B$ and $\sigma_B'$ represent the strength of constrained and unconstrained bainite respectively, $\sigma_M$ is the strength of martensite, and $V_B$ is the volume fraction of bainitic ferrite. Young and Bhadeshia's model and experimental data from Coldren et al.[24] have been applied to estimate the empirical constants in equation (2) for the harder phase (bainite + martensite).

On the other hand, the method used to estimate the strength of austenite assumes that the strength in the softer phase is the result of three strengthening contributions: the strength of pure austenite iron in a fully annealed condition, solid solution strengthening due to carbon, and solid solution strengthening due to substitutional solutes. Thus, true stress / true strain of the soft phase or austenite has been calculated using the estimated value of the strength and Bhadeshia and Edmonds' experimental hardness results.[8] Table 1 lists the derived values of $K$ and $n$ for the softer and harder phases.

The results of the inhomogeneous deformation analysis by Tomota's method, together with experimental tensile results are shown in Fig. 1 and Table 2 for Fe-0.2C-2Si-3Mn wt-% and Fe-0.4C-2Si-4Ni wt-% alloys which have been studied in

previous investigations.[8,9] A good agreement between experimental and calculated values of the maximum load has been found in the studied alloys. However, this model does not reproduce the low yield strength at the early stages of deformation caused by the presence of austenite in the microstructure.[25] This model could be therefore used to evaluate only the maximum load of any proposed alloy.

## 3 Design of new alloys

The aim of this work was to design bainitic alloys for defence application. Table 3 specifies the tensile and toughness properties required for that purpose. The engineering requirements are for a Charpy impact energy of 40 J at -40 $^{o}$C, a fracture toughness of 125 MPa$\sqrt{m}$, 1100 MPa tensile and 1000 MPa proof strength. A minimum ductility of 12% elongation and 50% reduction of area are also required.

Previous research, carried out by Bhadeshia and Edmonds[8,9] and Miihkinen and Edmonds[10-12], on two silicon-containing steels, nominally, Fe-0.2C-2Si-3Mn wt-% and Fe-0.4C-2Si-4Ni wt-% showed that these alloys hold promise. The Fe-0.2C-2Si-3Mn wt-% alloy exhibited excellent fracture toughness ($K_{Ic}$=160 MPa$\sqrt{m}$) in a strength range of 1375-1440 MPa as isothermally heat-treated at 250 $^{o}$C. This fracture toughness is better or equal than that of quenched and tempered AISI 300M and AISI 4340 steels at equivalent strength levels and approaches that of the 18 wt-% Ni maraging steel.[12] Because of the increased carbon content, higher strength levels 1500-1840 MPa were obtained in the Fe-0.4C-2Si-4Ni wt-% alloy, with lower fracture toughness values, but this still exceeded those of commercial high strength martensitic steels. The original experiments[8,9] were carried out in order to

demonstrate the role of the $T_o'$ curve in greatly influencing the mechanical properties of carbide-free bainitic steels. The experimental alloys developed for this purpose are not necessarily the optimum alloys from the point of view of mechanical properties. Our aim here was to use the combination of the models described above, to produce the best possible alloys, with microstructures produced by continuous cooling transformation, building on the previous work.[8,9]

Using the models together with some background knowledge, the following modifications were proposed to increase the maximum volume fraction of bainite in the final microstructure and to improve the hardenability of the steels:

- The silicon content was reduced to what is believed to be the minimum (1.5 wt-% Si) required to suppress carbide precipitation. This should lead to an improvement in the impact toughness, without deterioration in the $T_o'$ criterion or the hardenability.
- With the aim of increasing the strength of the Fe-0.2C-2Si-3Mn wt-% alloy, the carbon content was increased to 0.3 wt-% C with a reduction in the Mn content to 2 wt-% Mn in order to retain toughness. It was found that the $T_o'$ curve shifts to higher carbon when the Mn content is reduced. However, a reduction in manganese naturally reduces hardenability.
- In order to increase toughness of the Fe-0.4C-2Si-4Ni wt-% alloy, the amount of carbon was reduced to 0.3 wt-% C. Calculations show that the hardenability did not seem to change appreciably.
- Substantial improvements in both the strength and hardenability were obtained by adding 1.44 wt-% Cr to the nickel alloy. However, the $T_o'$ curve was found to shift to much lower carbon concentrations. Finally, Ni was reduced to 3.5 wt-%

Ni to increase the residual austenite carbon content without significantly sacrificing hardenability. For the manganese alloy, the best hardenability was achieved by adding 1.30 wt-% Cr without changes in Mn content.

– Commercial alloys inevitably contain phosphorus and other impurities. An addition of 0.25 wt-% Mo was made to reduce impurity embrittlement and to increase hardenability. This addition shifted the $T_o'$ curve to lower austenite carbon concentrations and hence the molybdenum was limited to 0.25 wt-%.
– Vanadium was added to restrict austenite grain growth during the austenitising heat treatment.

The alloys that have been proposed following a very large number of theoretical investigations, are listed in Table 4. Their compositions are expressed in weight percent. Figure 2 shows the calculated TTT diagrams representing the initiation of transformation. Also plotted are representative cooling curves[26] simply as an indication of hardenability. The curves should really be plotted on continuous cooling transformation diagrams, where the transformation curves would be displaced to longer times. The calculated microstructures listed in Fig. 2 are, on the other hand, rigorous, using the methods described in Refs. 27 and 28. In order to form a mixed microstructure of bainite and austenite by continuous cooling, it is necessary to avoid polygonal-ferrite and pearlite transformations. The diagrams suggest that the Ni1 and Ni2 alloys have enough hardenability if the steel is cooled in oil. In that case, the final microstructure in both steels is predicted to be 0.89 bainite and 0.11 austenite. Due to the high degree of transformation to bainite that takes place, the majority of the retained austenite is expected to be present as films between the sub-units of bainitic ferrite. This should result in a microstructure with

an optimum toughness. Furthermore, for the Mn alloy, a bainite-rich microstructure can be obtained by air cooling, but it is possible that some polygonal-ferrite may form. However, because of the slow kinetics at temperatures as low as 600 °C, it is likely that any polygonal-ferrite will be very limited. Likewise, Table 5 shows the tensile properties calculated using the deformation model described above. A very high strength is expected from the novel alloys.

## 4 Conclusions

In steels containing sufficient quantities of silicon, it is possible to obtain a microstructure consisting of a mixture of bainitic ferrite, carbon-enriched retained austenite and some martensite. The mechanism by which bainite grows, places strict limits on the temperature range for transformation and on the maximum fraction of transformation that can ever be achieved. These criteria are embedded in the concept of $T_o'$ curve. Thus, thermodynamic theory relying on the $T_o'$ concept has been used to design and optimum microstructure, which avoids large regions of austenite known to be detrimental for toughness.

At the same time, detailed kinetic theory has been used to ensure that the hardenability of the steel is sufficient for the specified industrial application and that the microstructure can be generated by continuous cooling transformation. A model for strength has been developed to guide the design process.

The compositions of Fe-0.2C-2Si-3Mn wt-% and Fe-0.4C-2Si-4Ni wt-% alloys from previous studies have been used to propose new alloys optimised with respect to strength and toughness. Three new alloys have been proposed as new high strength

bainitic steels. The theoretical design of their composition has been made through the knowledge of phase transformation theory.

## 5 Acknowledgments

This work was carried out as part of Technology Group 4 (Materials and Structures) of the MoD Corporate Research Programme. The authors would like to thank to Professor Alan Windle for the provision of laboratory facilities at the University of Cambridge.

## 6 References


1. S. J. MATAS and R. F. HEHEMANN: *Trans. Met. Soc. AIME*, 1961, **221**, 179-185.
2. R. ENTIN: in 'Decomposition of Austenite by Diffusional Processes', (ed. V. F. Zackay and H. I. Aaronson), 295-311; 1962, New York, Interscience.
3. R. F. HEHEMANN: in 'Phase Transformations', 397-432; 1970, Metals Park, Ohio, American Society for Metals.
4. T. LYMAN and A. R. TROIANO: *Trans. Met. Soc. AIME*, 1945, **162**, 196.
5. R. LEHOUILLIER, G. BEGIN, and A. DUBE: *Metall. Trans*., 1971, **2A**, 2645.
6. H. K. D. H. BHADESHIA and D. V. EDMONDS: *Metall. Trans*., 1979, **10A**, 895-907.
7. H. K. D. H. BHADESHIA and D. V. EDMONDS: *Acta Metall*., 1980, **28**, 1265-1273.
8. H. K. D. H. BHADESHIA and D. V. EDMONDS: *Metal Sci.,* 1983, **17**, , 411-419.
9. H. K. D. H. BHADESHIA and D. V. EDMONDS: *Metal Sci*., 1983, **17**, 420-425.
10. V. T. T. MIIHKINEN and D. V. EDMONDS: *Mater. Sci. Technol*., 1987, **3**, 422-431.
11. V. T. T. MIIHKINEN and D. V. EDMONDS: *Mater. Sci. Technol*., 1987, **3**, 432-440.
12. V. T. T. MIIHKINEN and D. V. EDMONDS: *Mater. Sci. Technol*., 1987, **3**, 441-449.
13. H. K. D. H. BHADESHIA: *Mater. Sci. Technol*., 1999, **15**, 22-29.
14. H. K. D. H. BHADESHIA: *Acta Metall*., 1981, **29**, 1117-1130.

15. H. K. D. H. BHADESHIA and A. R. WAUGH: *Acta Metall.*, 1982, **30**, 775-784.
16. L. C. CHANG and H. K .D. H. BHADESHIA: *Mater. Sci. Eng.*, 1994, A184, L17-20.
17. I. STARK, G. D. W. SMITH and H. K. D. H. BHADESHIA: in 'Solid→Solid Phase Transformations', (ed. G. W. Lorimer), 211-215; 1988, London, Institute of Metals.
18. H. K. D. H. BHADESHIA: *Metal Sci.*, 1982, **16**, 159-165.
19. G. E. DIETER: 'Mechanical Metallurgy', 138; 1961, New York, McGraw-Hill.
20. Y. SOYAMA: *J. Soc. Mater. Sci. Kyoto*, 1966, **15**, 17.
21. Y. TOMOTA, K. KUROKI and I. TAMURA: *J. Iron Steel Inst. of Japan*, 1975, **61**, 107.
22. Y. TOMOTA, K. KUROKI, T. MORI and I. TAMURA: *Mater. Sci. Eng.*, 1976, 24, 85-94.
23. C. H. YOUNG and H. K. D. H. BHADESHIA: *Mater. Sci. Technol.*, 1994, 10, 209-214.
24. A. P. COLDREN, R. L. CRYDERMAN and M. SEMCHYSHEN: 'Steel Strengthening Mechanisms', 17; 1969, Ann Arbor, USA, Climax Molybdenum.
25. B. P. J. SANDVIK and H. P. NEVALAINEN: *Met. Tech.*, 1981, **15**, 213-220.
26. Defence Evaluation Research Agency Technical Note, DRA/WSS/WT6/CR/93 2/1.0.
27. N. CHESTER and H. K. D. H. BHADESHIA: *Journal de Physique IV*, 1997, **7**, 41-46.
28. S. J. JONES and H. K. D. H. BHADESHIA: *Acta Materialia*, 1997, **45**, 2911-2920.

**Table 1 Values of $K$ and $n$ Considered in the Deformation Model**

| Alloy | $K_s$ / MPa | $K_h$ / MPa | $n_s$ | $n_h$ |
|---|---|---|---|---|
| Fe-0.2C-2Si-3Mn wt-% | 1254 | 2332 | 0.2 | 0.04 |
| Fe-0.4C-2Si-4Ni wt-% | 1558 | 2786 | 0.2 | 0.04 |

$K_s$ strength coefficient for the soft phase; $K_h$ strength coefficient for the hard phase; $n_s$ strain hardening coefficient for the soft phase; $n_h$ strain hardening coefficient for the hard phase.

**Table 2 Experimental and Predicted Mechanical Properties**

| Alloy | True Stress / MPa | | Maximum Load / MPa | |
|---|---|---|---|---|
| | Experimental | Predicted | Experimental | Predicted |
| Fe-0.2C-2Si-3Mn wt-% | 992 | 1383 | 1772 | 1788 |
| Fe-0.4C-2Si-4Ni wt-% | 1105 | 1192 | 2116 | 1959 |

**Table 3 Required Mechanical Properties for Defence Applications**

| YS | UTS | Elongation | RA | $CV_{-40\,°C}$ | $K_{IC}$ |
|---|---|---|---|---|---|
| MPa | MPa | % | % | Joules | MPa $\sqrt{m}$ |
| 1000 | 1100 | 12 | 50 | 40 | 125 |

YS yield strength; UTS ultimate tensile strength; RA reduction of area; CV impact energy; $K_{Ic}$ plane-strain fracture toughness.

**Table 4 Chemical Composition of Alloys Designed, wt-%**

| Alloy | C | Si | Mn | Ni | Cr | Mo | V |
|---|---|---|---|---|---|---|---|
| Mn | 0.30 | 1.5 | 2.00 | - | 1.30 | 0.25 | 0.1 |
| Ni1 | 0.30 | 1.5 | - | 3.5 | 1.44 | 0.25 | 0.1 |
| Ni2 | 0.30 | 1.5 | - | 3.5 | 1.44 | 0.25 | - |

**Table 5 Tensile Strength Expected from the Novel Alloys**

| Alloy | YS / MPa | UTS / MPa |
|---|---|---|
| Mn | 2271 | 2341 |
| Ni1 | 1634 | 2243 |
| Ni2 | 1964 | 2321 |

YS yield strength; UTS ultimate tensile strength.

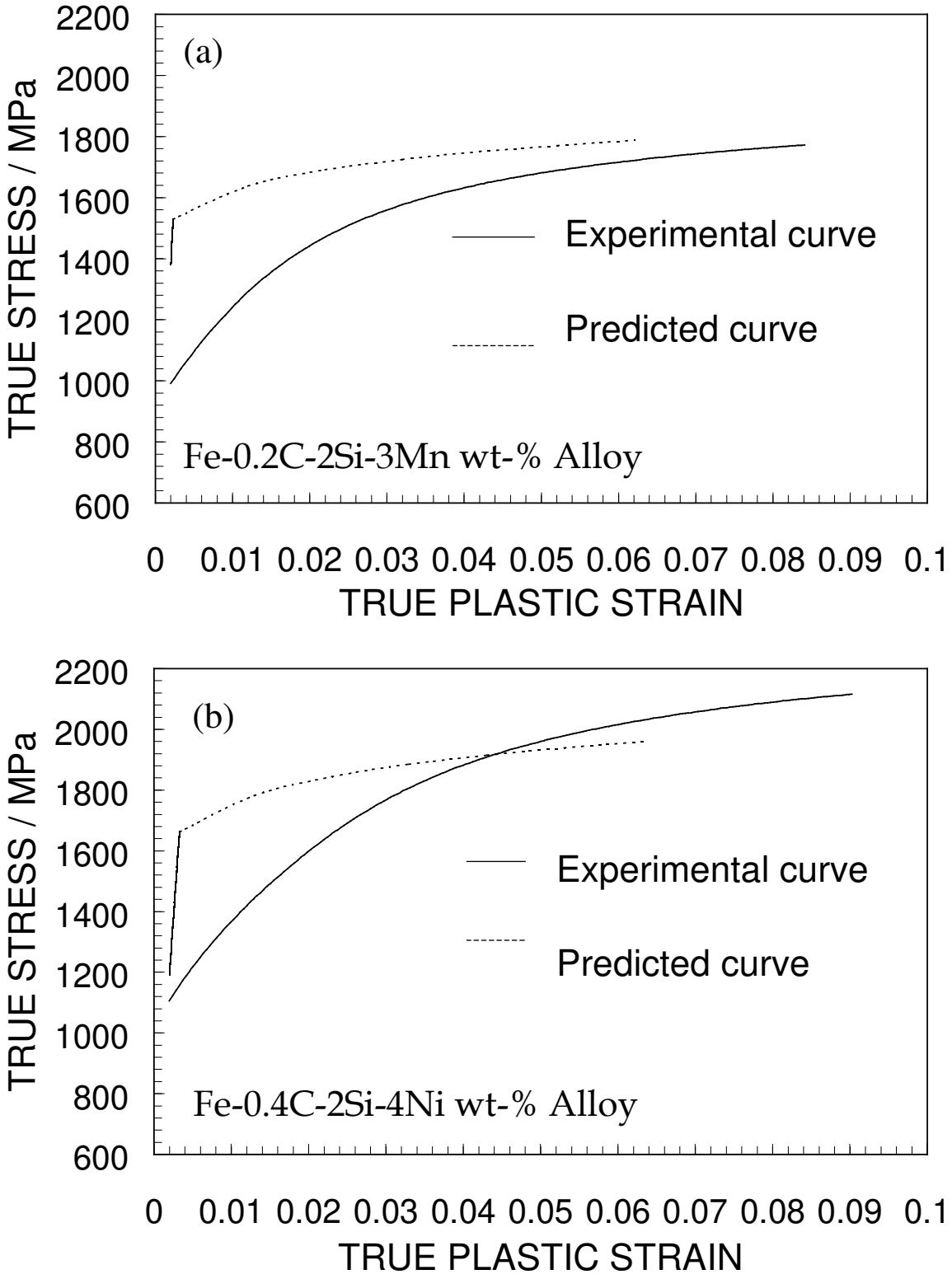


*a* Fe-0.2C-2Si-3Mn wt-% alloy; *b* Fe-0.2C-2Si-4Ni wt-% alloy

**1 Calculated and experimental true stress / true strain curves**

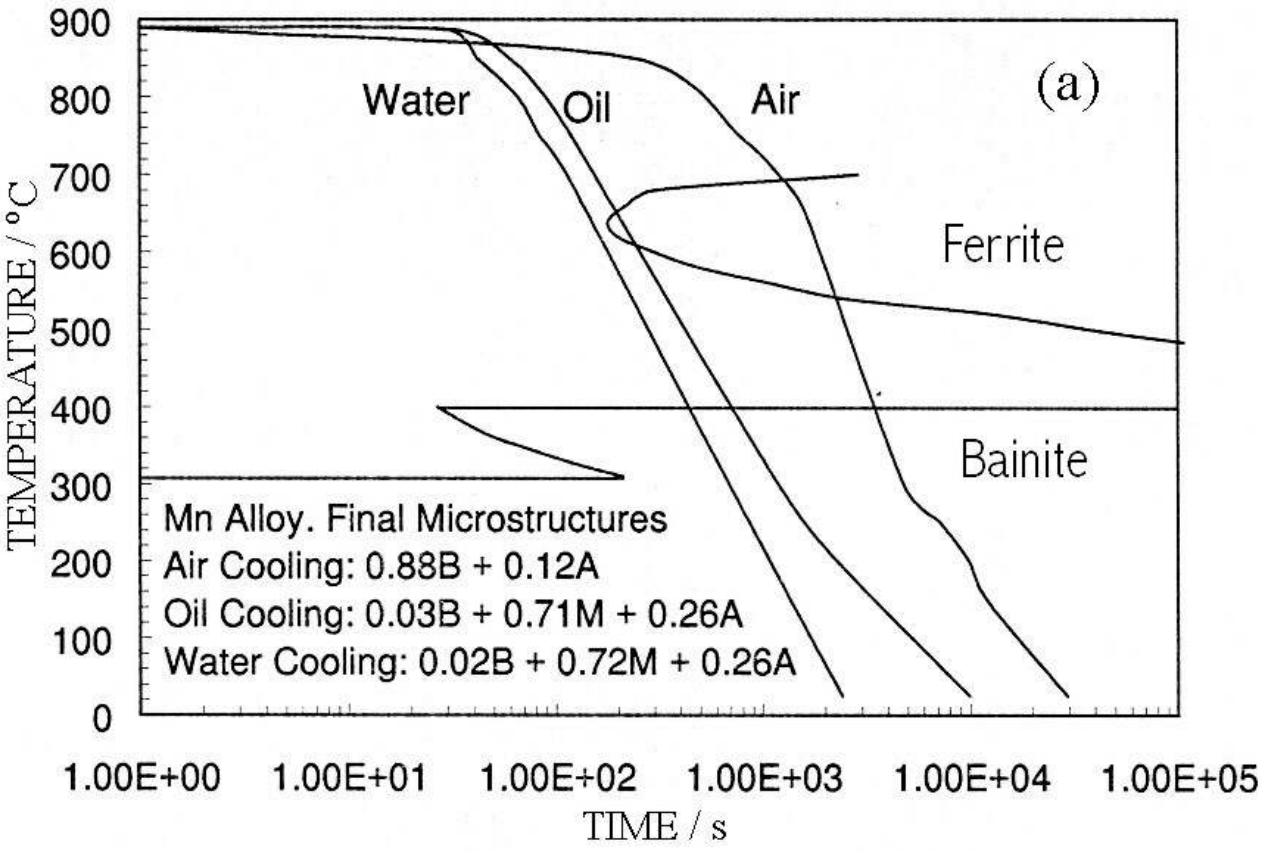
900
800
700
600
500
400
300
200
100
0
TEMPERATURE / °C
Water
Oil
Air
(a)
Ferrite
Bainite
Mn Alloy. Final Microstructures
Air Cooling: 0.88B + 0.12A
Oil Cooling: 0.03B + 0.71M + 0.26A
Water Cooling: 0.02B + 0.72M + 0.26A
1.00E+00
1.00E+01
1.00E+02
1.00E+03
1.00E+04
1.00E+05
TIME / s

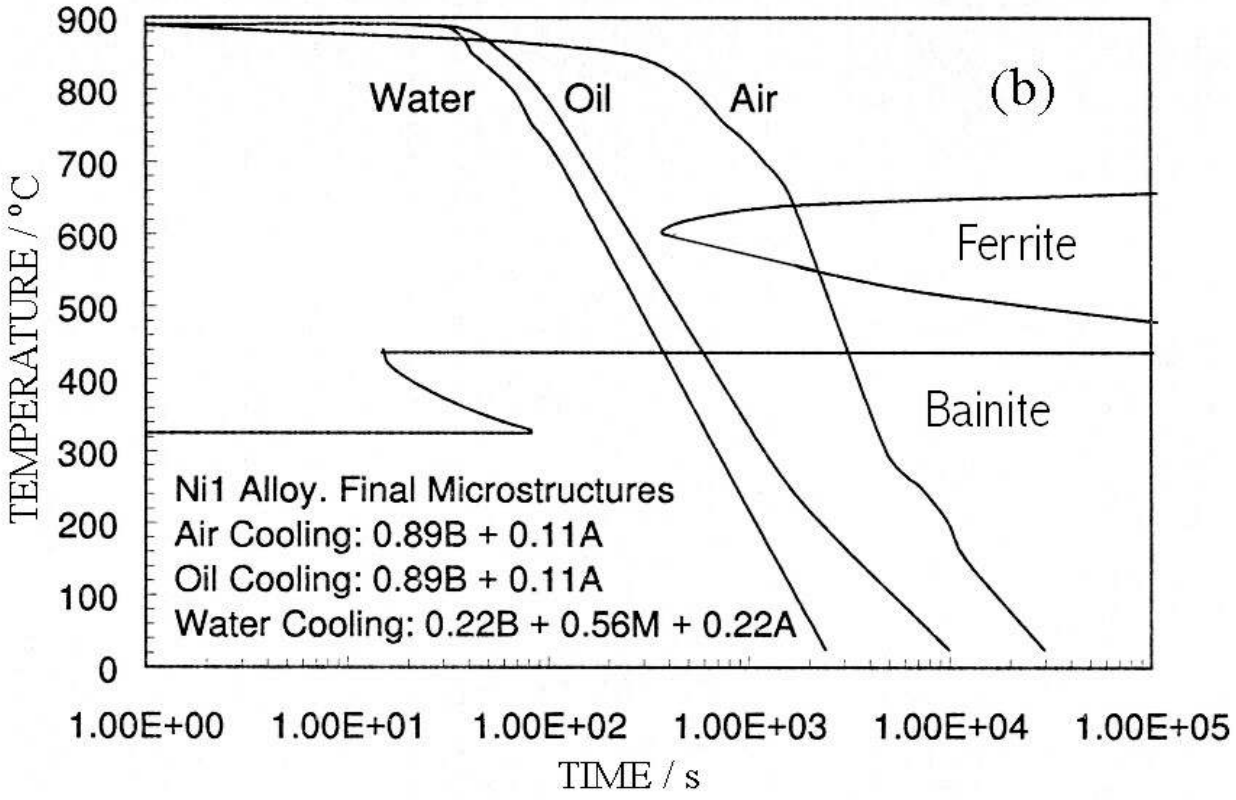
900
800
700
600
500
400
300
200
100
0
TEMPERATURE / °C
Water
Oil
Air
(b)
Ferrite
Bainite
Ni1 Alloy. Final Microstructures
Air Cooling: 0.89B + 0.11A
Oil Cooling: 0.89B + 0.11A
Water Cooling: 0.22B + 0.56M + 0.22A
1.00E+00
1.00E+01
1.00E+02
1.00E+03
1.00E+04
1.00E+05
TIME / s

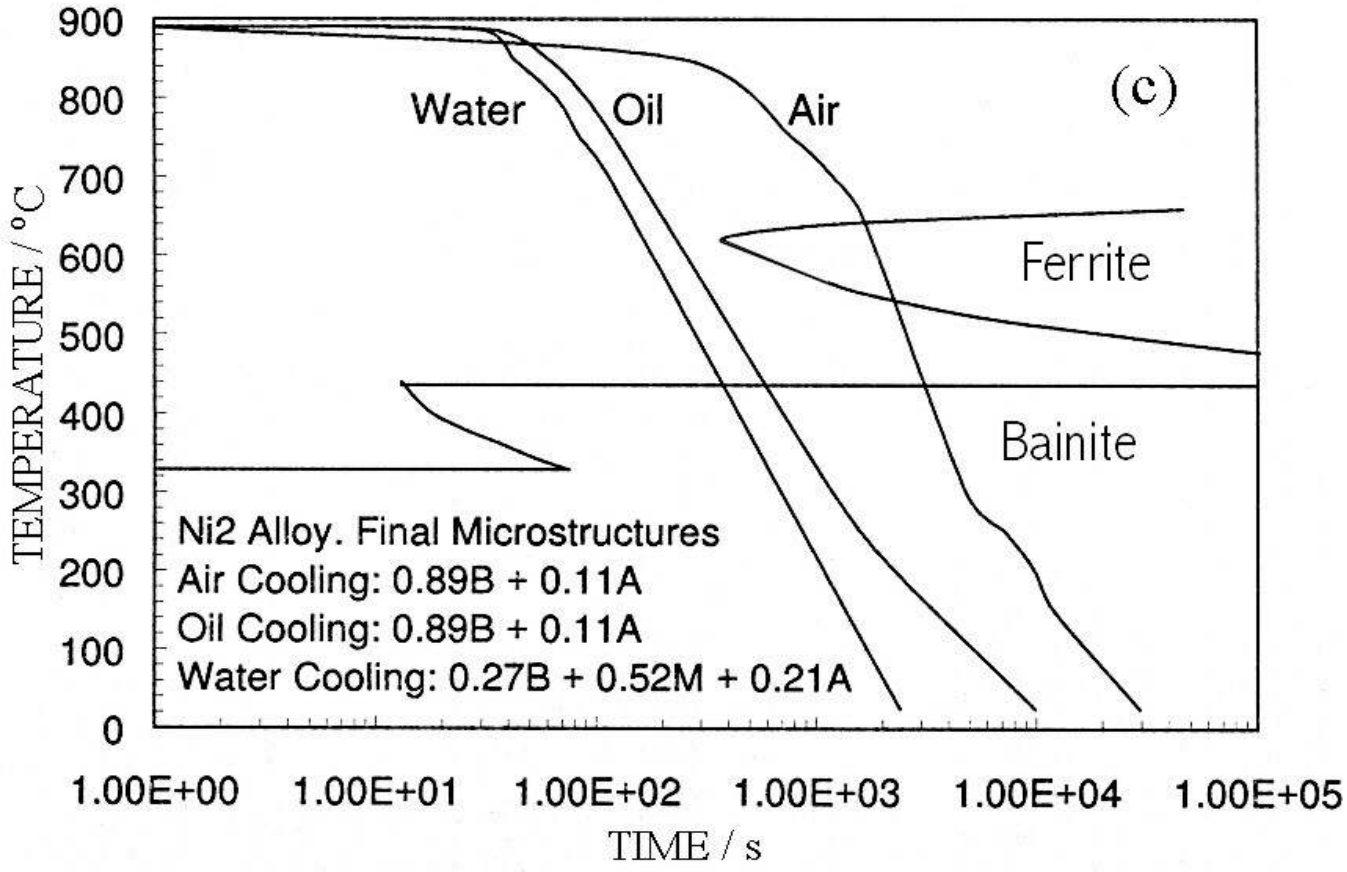


*a* Mn alloy; *b* Ni1 alloy; *c* Ni2 alloy

**2 Calculated TTT diagram for the initiation of transformation. The cooling curves are representative of the core of a steel bar of 210 mm diameter. They are superimposed on the TTT diagram simply as a rough indication of hardenability, since they should strictly be plotted on a continuous cooling transformation diagram. The legends B, M and A refer to bainite, martensite and austenite, respectively.**